Phases in antiferroelectric-side $Rb_{1-x}(ND_4)_xD_2AsO_4$ mixed crystals by light scattering

Chi-Shun Tu, S.-S. Gao, R.-J. Jaw, Z.-Q. Xue, and L.-G. Hwa
Department of Physics, Fu-Jen University, Taipei, Taiwan 242, Republic of China

V. Hugo Schmidt
Department of Physics, Montana State University, Bozeman, Montana 59717

(Received 20 February 1998)

The Raman spectra of A_1, B_2, and E symmetries and the longitudinal [100] Brillouin backscattering have been measured as a function of temperature in the mixed ferroelectric (FE)-antiferroelectric (AFE) system $Rb_{1-x}(ND_4)_xD_2AsO_4$ (DRADA-x) for ammonium concentrations $x=0.39$, 0.55, 0.69, and 1.0. Successive phase transitions [paraelectric (PE) phase→coexistence of PE and AFE phases→AFE phase] were observed in both $x=0.55$ and 0.69 as the temperature decreases. Taking into account earlier dielectric results, a phase coexistence of the deuteron-glass state and the AFE order is confirmed in $x=0.39$. In addition, a broad damping peak (that is associated with a Landau-Khalatnikov-like maximum in $x=0.55$ and 0.69) was observed in the Brillouin phonon spectra of $x=0.39$, 0.55, and 0.69. Such an anomaly is attributed to dynamic order-parameter fluctuations. Using previous results for ferroelectric-side DRADA-x, a phase diagram (ND_4 concentration x vs T) with qualitative phase boundaries is also given. [S0163-1829(98)09033-X]

I. INTRODUCTION

In the mixed ferroelectric-antiferroelectric (FE-AFE) system $A_{1-x}(ND_4)_xD_2BO_4$ [A=Rb (or K, Cs) and B=As (or P)], there is competition between FE and AFE orderings, each characterized by specific configurations of the acid deuterons.[1–8] The random distribution of the Rb and ND_4 ions is the main source to produce frustration that can increase local structural competition such that the long-range electric order disappears. Instead of a typical sharp FE or AFE phase transition, phase coexistence (such as PE/FE and PE/AFE) becomes a characteristic of such mixed compounds. As an example, in $Rb_{0.9}(ND_4)_{0.1}D_2AsO_4$ the short-range antiferroelectric order due to freezing-in of the ND_4 reorientations and associated O–D···O ''acid'' deuteron bond rearrangement is responsible for FE/PE phase coexistence as evidenced by gradual changes with temperature seen in dielectric, NMR, and light-scattering results.[2–5]

By a group-theory analysis for the potassium dihydrogen phosphate (KH_2PO_4)-type structure (that contains two molecular units in a primitive unit cell) at zero wave vector, the vibrational modes in the tetragonal symmetry (space group $I\bar{4}2d$-D_{2d}^{12}) can be decomposed into the following irreducible representations: $\Gamma_{vib}=4A_1(R)+5A_2(\text{silent})+6B_1(R)+6B_2(R,IR)+12E(R,IR)$.[9] The symmetry species A_1, B_1, B_2, and E are Raman active. The situation in the mixed system DRADA-x is more complicated than in the parent crystals, because some Rb (or ND_4) ions have been substituted by ND_4 (or Rb) ions. In this case, the selection rule of the free AsO_4 group is expected to be broken much more easily than in the pure crystal. In other words, the local site symmetry of the AsO_4 group is anticipated to be lower as compared with the parent crystals.

In recent years, many measurements in the DRADA-x system have been made on ferroelectric-side crystals such as $x=0$, 0.10, and 0.28.[2–5] The vibrational frequencies of the in-plane bending mode δ(O-D) and the AsO_4 group were also assigned.[5] However, only few experiments were done on antiferroelectric-side compounds ($x\geqslant 0.35$).[6,7] Complete understanding of this mixed system is still lacking. This motivated us to carry out both polarized Raman and Brillouin light scattering on DRADA ($x=0.39$, 0.55, 0.69, and 1.0). Here, we pay special attention to the temperature dependences of the symmetric stretching mode ν_1 (near 755 cm^{-1}) of the AsO_4 group and the in-plane bending mode δ(O-D) (near 825 cm^{-1}) measured from the B_2-$y(xy)x$ configuration. Also, these results will be compared with the temperature dependences of acoustic phonon frequency and half width from the Brillouin near backscattering. In particular, a phase diagram (ND_4 concentration x vs T) will be presented.

II. EXPERIMENTAL PROCEDURE

Single crystals of $Rb_{1-x}(ND_4)_xD_2AsO_4$ ($x=0.39$, 0.55, 0.69, and 1.0) were grown from aqueous solutions with certain ratios of RbD_2AsO_4 (DRDA) and $ND_4D_2AsO_4$ (DADA) by slow evaporation of D_2O in an atmosphere of argon gas. The ND_4 concentrations were determined from the ratio of Rb and N atoms by x-ray photoelectron spectroscopy. The relation of ND_4 concentration between x' (in solution) and x (in crystal) is linear within experimental error ($\pm 3\%$). The green light with $\lambda=514.5$ nm from an argon ion laser was used as an excitation source. The laser power incident on the samples was kept less than 150 mW. For Raman measurements, an ISA Model U1000 double grating monochromator equipped with a water cooled photomultiplier detector was used. Right-angle spectra were taken from scattering geometries $y(zz)x$, $y(xy)x$, and $y(xz)x$ that correspond to A_1, B_2, and E symmetries, respectively. Here x, y, and z relate to the crystal a, b, and c axes, respectively. A Janis VPF-100 variable temperature pourfill cryostat was used with a Lake-Shore Model 321 temperature controller.

The Brillouin phonon spectra were obtained from the near backscattering with configuration $x(zu)\bar{x}$. ''u'' means that the collection was not polarization discriminated. The

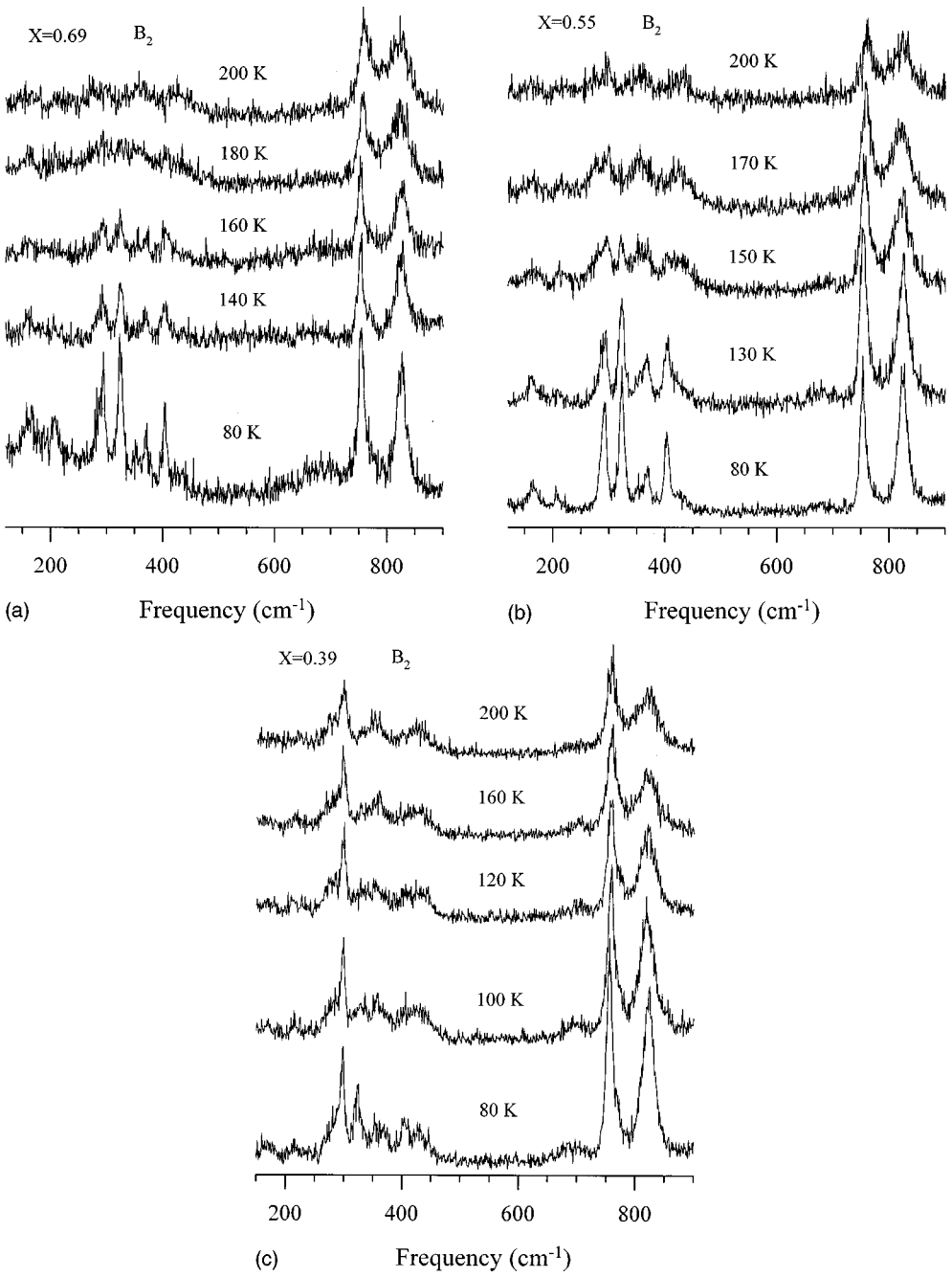

FIG. 1. Temperature-dependent Raman spectra ($50-10^3$ cm^{-1}) of DRADA (a) $x=0.69$, (b) $x=0.55$, and (c) $x=0.39$ measured from the B_2-$y(xy)x$ geometry.

samples were illuminated along [100], so the longitudinal acoustic (LA) phonons with wave vector along [100] were studied. According to the theoretical calculation for a tetragonal structure, there should be no transverse acoustic (TA) mode to be expected in the case of backscattering due to a weak intensity factor.[10] Scattered light was analyzed by a Burleigh five-pass Fabry-Perot interferometer. To improve the spectral resolution, the Brillouin doublet was adjusted to appear in the second order with respect to the Rayleigh line. In our experiments, the free spectral range (FSR) of the Fabry-Perot is determined by measuring the LA phonon shift of fused quartz. The free spectral range was 20.63 GHz for the spectra of this paper. A Janis CCS-150 closed cycle refrigerator was used with a LakeShore Model 340 temperature controller.

To determine the accurate positions and half widths of both the Raman and Brillouin components, the damped harmonic oscillator model with the spectral response function[11]

$$S(\omega)=\frac{\chi_0\Gamma\omega\omega_0^2}{(\omega^2-\omega_0^2)^2+\Gamma^2\omega^2}\,\frac{1}{1-e^{-\hbar\omega/kT}}, \tag{1}$$

was used, where ω_0 and $\Gamma_{\rm obs}$ correspond to the phonon frequency and observed half width, respectively, χ_0 is the susceptibility constant (in arbitrary units), k is Boltzmann's constant, and T is the absolute temperature. For Brillouin backscattering, the broadening due to collection optics is negligible.[12] In this case, the natural-phonon half width $\Gamma_{\rm ph}$ is given by $\Gamma_{\rm ph}=\Gamma_{\rm obs}-\Gamma_{\rm inst}$.[3] In our experiments, the half

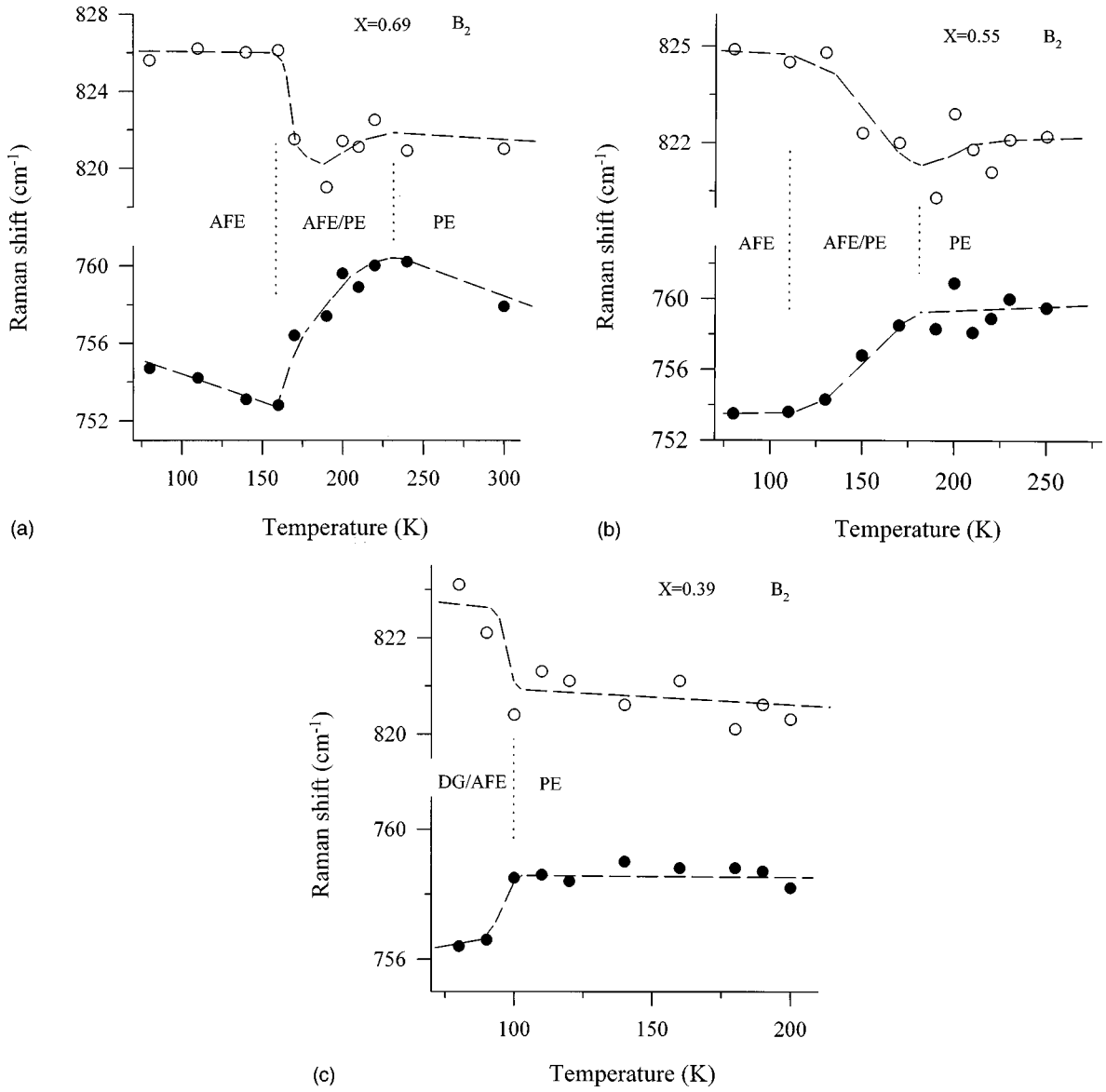

FIG. 2. Frequency vs temperature variations of two Raman vibrations (measured from the B_2 symmetry) of DRADA (a) $x=0.69$, (b) $x=0.55$, and (c) $x=0.39$. These two modes correspond to the in-plane bending mode $\delta(O\text{-}D)$ (open circle) and the stretching mode ν_1 (solid circle) of the AsO_4 group. The dashed lines are guides for the eye and the dotted lines are the estimates of various phase boundaries.

width of the laser line (for $\lambda=514.5$ nm) is about 0.02 GHz, determined by the spectrometer. The half width of the Rayleigh line from fused quartz (that was assumed to have a Gaussian profile) was taken as the instrumental broadening $\Gamma_{inst}\sim 0.007$ FSR.

III. RESULTS AND DISCUSSION

Actual temperature-dependent B_2-$y(xy)x$ Raman spectra are shown in Figs. 1(a)–1(c) for $x=0.69$, 0.55, and 0.39, respectively. All three compounds display a similar Raman pattern and high scattering efficiency in the high-frequency region (720–850 cm^{-1}). However, at low frequency (<500 cm^{-1}), $x=0.39$ shows different vibrational components as compared to $x=0.69$ and 0.55. Specifically, the Raman spectra of $x=0.39$ do not show any apparent difference as temperature changes. The main Raman lines observed from the B_2 configuration are at frequencies near 290, 320, 400, 760, and 820 cm^{-1}.

The temperature dependences of the in-plane bending mode δ(O-D) (near 825 cm^{-1}) and the stretching mode ν_1 (near 760 cm^{-1}) of the AsO_4 group from the B_2 symmetry for $x=0.69$, 0.55, and 0.39, are plotted in Figs. 2(a)–2(c), respectively. As temperature decreases, the δ(O-D) modes of both $x=0.69$ and 0.55 show a notable hardening (that is more progressive in $x=0.55$). On the contrary, the stretching modes ν_1 (near 760 cm^{-1}) display a gradual softening that begins at $T\sim 230$ and ~ 180 K and ends at $T\sim 160$ and ~ 110 K in $x=0.69$ and 0.55, respectively. Instead of a slow rising, abrupt step-up and step-down behavior (at ~ 100 K) were observed in the δ(O-D) and ν_1 modes in $x=0.39$, respectively.

Figures 3(a)–3(c) show the actual LA[100] phonon spectra of the anti-Stokes Brillouin component for $x=0.69$, 0.55, and 0.39, respectively. The data shown here are for several temperatures near the maximum value of half width. The solid lines are fits of Eq. (1), from which the frequency shift and half width Γ_{obs} were obtained. Figures 4(a)–4(c) display

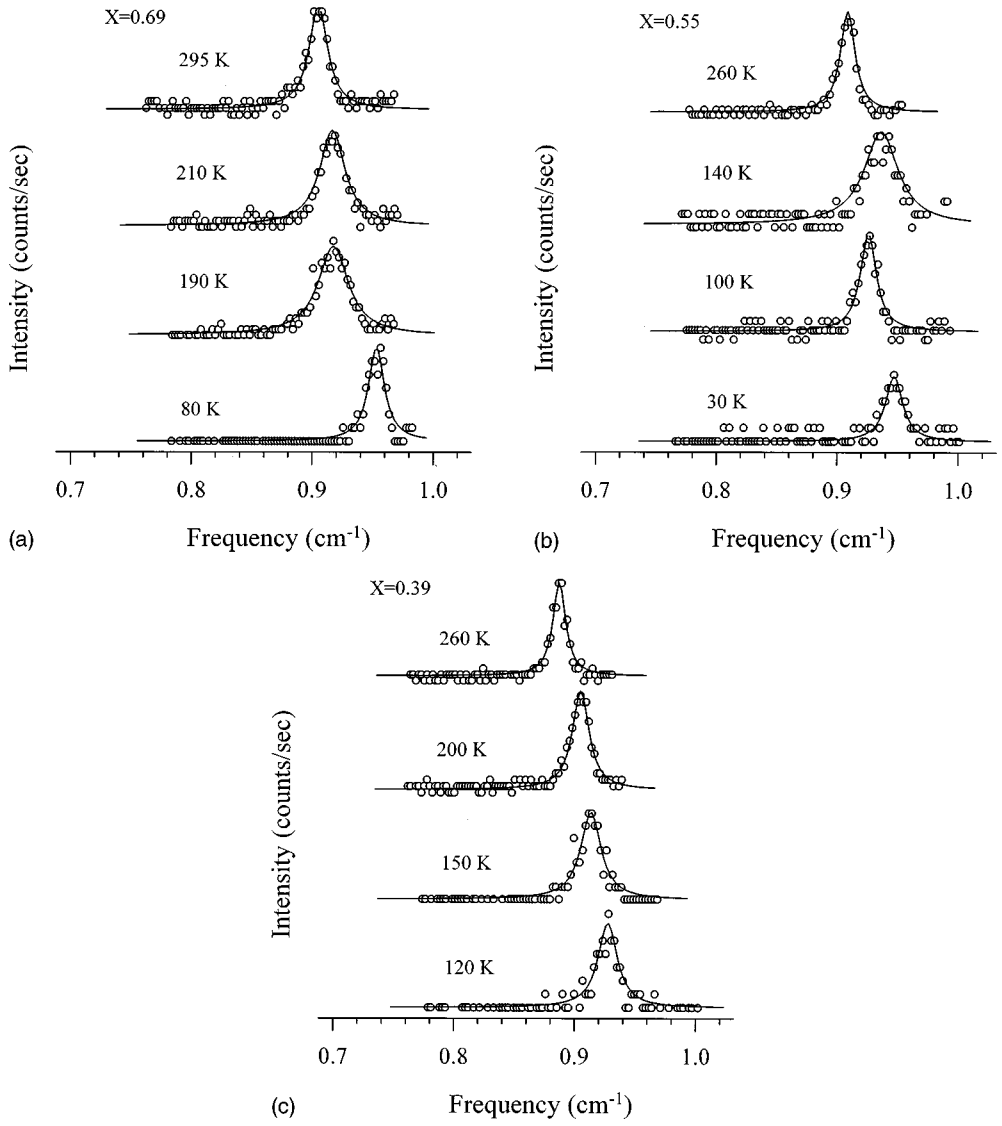

FIG. 3. Anti-Stokes components of the LA[100] Brillouin phonon spectra for temperatures around the maximum value of half width for (a) $x=0.69$, (b) $x=0.55$, and (c) $x=0.39$. The open circles are the measured data and solid lines are fits of Eq. (1).

the temperature dependences of the frequency shift and half width Γ_{ph}. The phonon frequency increases as ammonium concentration increases due to the lighter molecular mass of ND_4 ion. With increasing temperature, the phonon frequencies of all compounds exhibit a softening (that shows an almost linear curve in $x=0.39$). The damping data of Figs. 4(a)–4(c) exhibit a gradual growth and reach a broad maximum near 230, 180, and 140 K for $x=0.69$, 0.55, and 0.39, respectively. Such a development of damping must be associated with the order-parameter fluctuations that are characteristic of an $\eta^2\mu$-type coupling, squared in order parameter and linear in strain.[13] An additional sharp peak (that can be connected with the Landau-Khalatnikov maximum) was also observed near 190 and 140 K in $x=0.69$ and 0.55, respectively. The Landau-Khalatnikov maximum usually occurs near T_c and can be used as an indication of a long-range order FE or AFE phase transition.[3,13,14]

To determine the relation between phase characteristic and ammonium concentration, the low-temperature spectra from scattering geometries A_1-$y(zz)x$ and E-$y(xz)x$ were measured for $x=1.0$, 0.69, 0.55, and 0.39, and are given in Figs. 5(a)–5(b), respectively. Figure 5(c) shows a comparison of the B_2 spectra. The main vibrations of the A_1, B_2, and E symmetries are summarized in Table I. The stretching mode ν_1 (near 750 cm^{-1}) of the AsO_4 group is nondegenerate with only A_1 symmetry.[15] However, as shown in Figs. 5(a)–5(c) and Table I, the leakage of the ν_1 mode into the E and B_2 symmetries is practically as strong as the permitted vibrations. The ν_1 leakage that occurs in both the E and B_2 configurations is possible as the result of the lowering of local symmetry of the AsO_4 groups from S_4 to C_2 or even to C_1. Another interesting feature (as seen in Table I) is that a frequency doublet with a narrow splitting of about 10 cm^{-1} was observed in the ν_1 modes of the A_1, B_2, and E geometries for all samples. A possible reason for this splitting is that different AsO_4 groups have different combinations of surrounding ions, which will cause slight perturbation to the ν_1 frequency. A similar symmetry leakage was also observed in the doubly degenerate bending modes ν_2 (near 290 and 325 cm^{-1}) of the AsO_4 group, which should be observed in the A_1 and B_2 modes if the AsO_4 group has S_4 site symmetry.

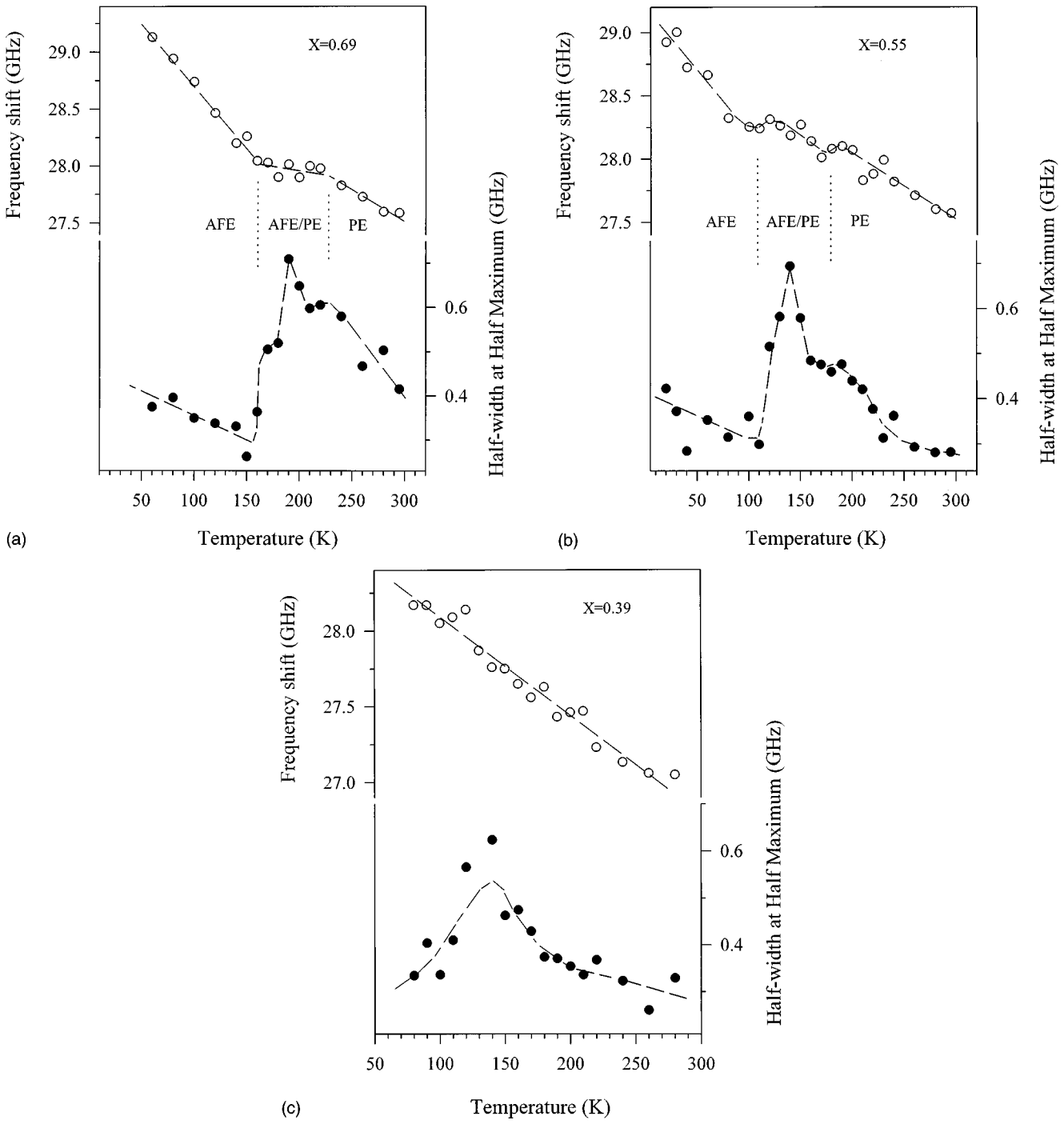

FIG. 4. Brillouin shift (open circle) and half width Γ_{ph} (solid circle) vs temperature of the LA[100] phonons for (a) $x=0.69$, (b) $x=0.55$, and (c) $x=0.39$. The dashed lines are guides to the eye and the dotted lines are the estimates of various phase boundaries.

What are the origins of these temperature-dependent phenomena shown in Figs. 2(a) and 4(a) for $x=0.69$? With decreasing temperature, the stretching mode ν_1 (near 755 cm^{-1}) of $x=0.69$ begins a gradual softening near 230 K and then reaches a minimum at ~160 K. The ν_1 mode is sensitive to the deuteron ordering near the AsO_4 group. In other words, if the deuteron arrangement modulates with temperature, the mass and force constants of the D_2AsO_4 group will be changed and thus influence the ν_1 frequency. As shown in Figs. 5(a)–5(c), $x=0.69$ has a Raman pattern similar to pure DADA in the low-temperature region. In addition, the half width of the δ(O-D) mode (near 824 cm^{-1}) becomes much broader as $T>\sim 160$ K [see Fig. 1(a)]. The ν_2 mode (near 325 cm^{-1}), which is the strongest component in the low-frequency region (<500 cm^{-1}) of DADA, also shows up apparently at $T\sim 160$ K. The acoustic damping [shown in Fig. 4(a)] also has an abrupt drop and reaches a minimum near 160 K. Thus, one can conclude that $x=0.69$ possesses an AFE ordering below $T\sim 160$ K. What does the progressive softening (that begins at ~230 K and ends at ~160 K) of the ν_1 mode mean? Comparison can be made to earlier Brillouin scattering results from the ferroelectric-side DRADA-x system,[3] in which a similar acoustic damping anomaly (a broad maximum associated with a sharp peak)

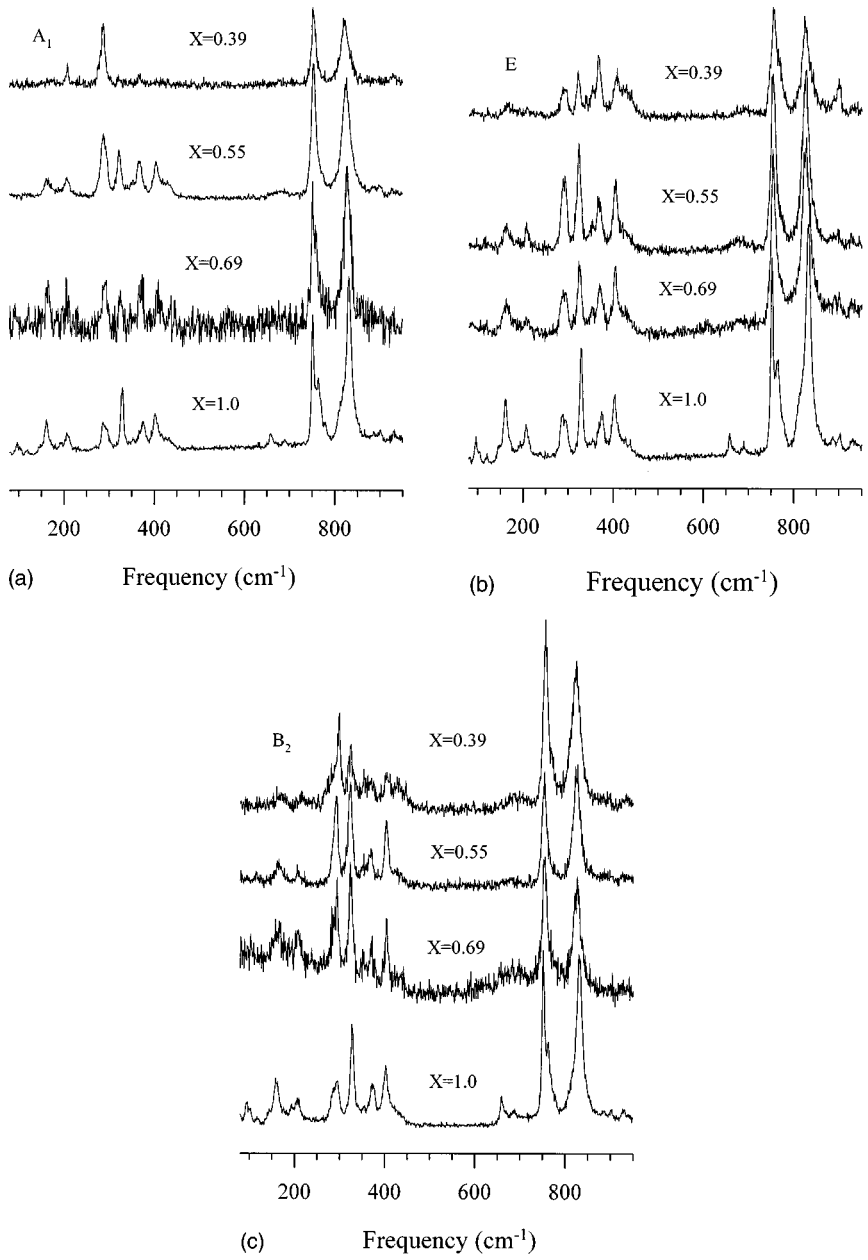

FIG. 5. Raman spectra of the (a) A_1-$y(zz)x$, (b) E-$y(xz)x$, and (c) B_2-$y(xy)x$ symmetries measured at 80 K (for $x=0.69$, 0.55, and 0.39) and 100 K (for DADA).

was observed in DRADA-0.10.[3] It was connected to a PE/FE phase coexistence due to the freezing-in of ND_4 reorientations associated with local destruction of FE ordering DRADA-0.10. For DRADA-0.69, one can expect that the partial replacement of ND_4 molecular groups by Rb atoms can cause growth of local structural competition (between FE and AFE orderings), so that long-range AFE ordering could be suppressed. In other words, neither a pure AFE nor PE phase but rather a PE/AFE phase coexistence will develop with decreasing temperature. As in DRADA-0.10, the broad damping maximum, centered at $T_m \sim 230$ K in DRADA-0.69, can be linked to the onset of phase coexistence of the PE/AFE type in this case. Moreover, the acoustic-phonon frequency [Fig. 4(a)] also exhibits successive slope changes at ~230 and ~160 K as the temperature decreases. In addition, the Landau-Khalatnikov maximum centered at ~190 K (that also corresponds to an abrupt drop in the ν_1 mode) is an evidence of a rapid growth of the AFE ordering. On the whole, one can conclude that PE/AFE phase coexistence begins at $T_m \sim 230$ K and then the crystal has a rapid growth of AFE ordering at ~190 K. Below $T \sim 160$ K, the AFE ordering becomes completely dominant in the $x=0.69$ crystal.

As shown in Fig. 2(b), an even smoother softening in the ν_1 mode was observed for $x=0.55$. This gradual declining behavior begins at $T \sim 180$ K and reaches a turning point at $T \sim 110$ K. The δ(O-D) mode also exhibits a gradual hardening that initiates at $T \sim 180$ K and ends at $T \sim 110$ K. As seen in Figs 5(a)–5(c), all the A_1, B_2, and E symmetries of $x=0.55$ have a similar Raman spectra like those of pure DADA in the low-temperature region. In addition, the ν_2 mode (near 325 cm^{-1}), which is the main vibration in the low-frequency region (<500 cm^{-1}) of pure DADA, also grows dramatically near 130 K [see Fig. 1(b)]. The acoustic

TABLE I. Frequencies of observed Raman modes (in cm^{-1}) in DRADA ($x=1.0$, 0.69, 0.55, and 0.39). The spectra were obtained at $T=80$ K (for $x=0.69$, 0.55, 0.39) and 100 K (for DADA).

B_2-$y(xy)x$				E-$y(xz)x$				A_1-$y(zz)x$			
1.0	0.69	0.55	0.39	1.0	0.69	0.55	0.39	1.0	0.69	0.55	0.39
832				832				832			
829	826	825	823	813	827	826	826	814	828	826	825
762	771	762	771	765	765	768	768	764	758	768	768
752	754	753	756	752	754	754	755	752	751	754	756
689	686		687	690			698	691		678	
660				659		676		659			
423		429	432	425	426	427	429	427	410	429	
402	404	404	404	403	404	404	407	403		405	
374	370	368	361	374	369	368	368	375	370	368	368
353		352		353		352	353	353		350	
328	324	323	324	329	325	323	322	329	327	323	325
295	294	291	298	296	290	290	290	290	290	289	289
285	287		285	287							279
207	209	207		208	208	208		207	207	207	208
203				192							
160	162	165		172	163	164		162	163	165	
142				161							
				146							

damping also has an abrupt drop and reaches a minimum near 110 K [see Fig. 4(b)]. Thus, one can conclude that the $x=0.55$ crystal has complete AFE ordering below $T\sim110$ K. What are the origins of the progressive softening and hardening (that begins at ~180 K and ends at ~110 K) in the ν_1 mode and the δ(O-D) mode, respectively? An acoustic damping anomaly similar to that for $x=0.69$ was also observed in DRADA-0.55. Such a broad damping maximum centered at $T_m\sim180$ K can be connect to the onset of formation of PE/AFE phase coexistence as for $x=0.69$. An additional Landau-Khalatnikov maximum centered at ~140 K was also observed and reveals a rapid growth of the AFE ordering near 140 K. Besides, the temperature dependency of the acoustic-phonon frequency also exhibits successive anomalies (two slight plunges) at ~180 and ~110 K with decreasing temperature [see Fig. 4(b)]. Thus, it is reasonable to conclude that $x=0.55$ exhibits PE/AFE phase coexistence which begins to form at $T_m\sim180$ K, and then has rapid growth of the AFE ordering at ~140 K. Below $T\sim110$ K, the AFE ordering becomes completely dominant in $x=0.55$.

For $x=0.39$, instead of a smooth rising, a step-up hardening and step-down softening were observed at $T\sim100$ K in the in-plane bending mode δ(O-D) (near 821 cm^{-1}) and the stretching mode ν_1 (near 758 cm^{-1}), respectively [see Fig. 2(c)]. As shown in Figs. 5(b) and 5(c), $x=0.39$ has similar Raman spectra with $x=1.0$, 0.69, and 0.55 in both the E and B_2 configurations in the low-temperature region. However, the A_1 symmetry of $x=0.39$ shows an apparent different spectrum compared with the A_1 spectra of $x=0.55$, 0.69, and 1.0 in the low-frequency region (<500 cm^{-1}). As seen in Fig. 5(a), only two clear vibrations (~290 and ~210 cm^{-1}) of the AsO_4 group are left in the low-frequency region. It implies that the long-range-order antiferroelectric phase somehow has been modified in the low-temperature region in $x=0.39$. Another important feature in $x=0.39$ is that its B_2 Raman spectra do not show any obvious change from 80 K up to room temperature [see Fig. 1(c)]. Also, the temperature dependency of the acoustic-phonon frequency [Fig. 4(c)] does not show any apparent anomaly. These phenomena indicate that the crystal structure is essentially the same in the temperature region ($300\geqslant T\geqslant80$ K). Furthermore, the acoustic damping shows a gradual growth (without the Landau-Khalatnikov maximum) and has a rough maximum near 140 K. Such an acoustic damping anomaly is similar to DRADA-$x=0.28$ and suggests the existence of a glass state (short-range order in cluster). The earlier dielectric results (ε' and ε'') of $x=0.39$ obtained by Trybula, Stankowski, and Los showed a frequency dispersion below ~100 K.[6] Two different relaxation mechanisms which were found by fitting the experimental data with two gaussian-shape curves, were attributed to a phase coexistence of deuteron-glass

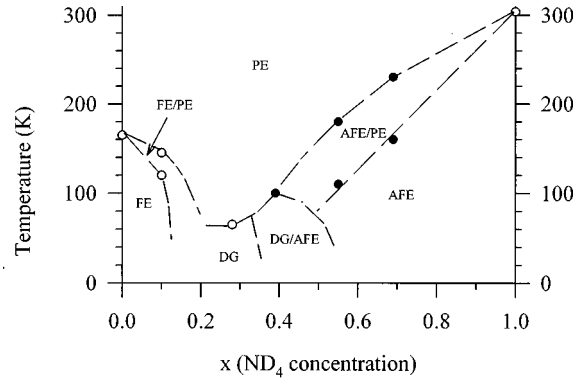

FIG. 6. Phase diagram (ND_4 concentration vs T) for the DRADA-x system. The dashed lines are estimates of various phase boundaries. The solid circles are the measured data from this present work and open circles are from Refs. 2–7 and 16.

(DG) state and antiferroelectric order. Thus, one can expect that the differences between the A_1 and B_2 (or E) spectra ($<500\ \mathrm{cm}^{-1}$) in $x=0.39$ can be related to two distinct local structural orderings. We conclude that the two breaks (at $T\sim100$ K) in both the δ(O-D) and ν_1 modes [see Fig. 2(c)] indicate the onset of DG/AFE phase coexistence.

With the previous NMR, dielectric, and Brillouin scattering results of DRADA ($x=0$, 0.10, 0.28, 0.39, and 1.0),[2–7,16] a phase diagram (ammonium concentration x vs temperature) is plotted in Fig. 6. The dashed lines are qualitative estimates of various phase boundaries. Such an asymmetric phase diagram verifies that the ND_4 ion has a stronger ordering effect than the Rb ion in the DRADA-x system.

IV. CONCLUSIONS

From the temperature-dependent Raman and Brillouin spectra of DRADA-1.0, 0.69, 0.55, and 0.39, three important features have been revealed in this report: (i) With decreasing temperature, successive phase transitions (PE ordering→PE/AFE phase coexistence→AFE ordering) are confirmed in both $x=0.55$ and 0.69. Instead of a PE/AFE coexistence, $x=0.39$ shows a DG/AFE phase coexistence taking place at $T\sim100$ K; (ii) the Raman spectra of the A_1, B_2, and E species exhibit a strong symmetry leakage possibly due to the lowering of local site symmetry of the AsO_4 group, and (iii) the phase diagram of DRADA-x is much more asymmetric as compared to that of $RB_{1-x}(NH_4)_xH_2PO_4$ (RADP).[8] Based on the present results, we propose that the DG state should exist for the ammonium concentration range of $0.2\leqslant x<0.39$.

ACKNOWLEDGMENTS

The authors would like to express sincere thanks to Dan Brandt for crystal growth. This work was supported by NSC Grant Nos. NSC86-2112-M-030-002 and NSC87-2112-M-030-001, and NSF Grant No. DMR-9520251.

[1] V. H. Schmidt, S. Waplak, S. Hutton, and P. Schnackenbeg, Phys. Rev. B **30**, 2795 (1984).
[2] N. J. Pinto, F. L. Howell, and V. H. Schmidt, Phys. Rev. B **48**, 5983 (1993).
[3] C.-S. Tu, and V. H. Schmidt, Phys. Rev. B **50**, 16 167 (1994).
[4] N. J. Pinto, Ph.D. thesis, Montana State University, 1993.
[5] C.-S. Tu, R.-M. Chien, and V. H. Schmidt, Phys. Rev. B **55**, 2920 (1997).
[6] Z. Trybula, J. Stankowski, and S. Los, Physica B **191**, 312 (1993).
[7] Z. Trybula, S. Waplak, J. Stankowski, S. Los, V. H. Schmidt, and J. E. Drumheller, Ferroelectrics **156**, 371 (1994).
[8] E. Courtens, Ferroelectrics **72**, 229 (1987).
[9] M. S. Shur, Kristallografiya **11**, 448 (1966) [Sov. Phys. Crystallogr. **11**, 394 (1966)].
[10] R. Vacher and L. Boyer, Phys. Rev. B **6**, 639 (1972).
[11] J. F. Ryan, R. S. Katiyar, and W. Taylor, Effet Raman et Théorie **C2**, 49 (1971).
[12] H. G. Danielmeyer, J. Acoust. Soc. Am. **47**, 151 (1970).
[13] W. Rehwald, Adv. Phys. **22**, 721 (1973).
[14] T. Hikita, P. Schnackenberg, and V. H. Schmidt, Phys. Rev. B **31**, 299 (1985).
[15] G. Herzberg, *Infrared and Raman Spectra of Polyatomic Molecules* (Van Nostrand, Princeton, NJ, 1945).
[16] C. Kittel, *Introduction to Solid State Physics*, 6th ed. (Wiley, New York, 1976), p. 386.